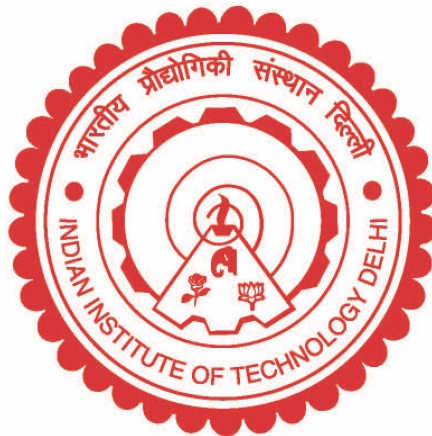


**DESIGN, DEVELOPMENT AND CONTROL OF  
BATTERY-SOLAR-WIND BASED HYBRID  
MICROGRID WITH SYNCHRONIZATION TO GRID**

**SUDIP BHATTACHARYYA**



**DEPARTMENT OF ELECTRICAL ENGINEERING  
INDIAN INSTITUTE OF TECHNOLOGY DELHI  
JUNE 2025**

© Indian Institute of Technology Delhi (IITD), 2025

# **Design, Development and Control of Battery-Solar-Wind Based Hybrid Microgrid with Synchronization to Grid**

by

**SUDIP BHATTACHARYYA**

**Electrical Engineering Department**

*Submitted*

*in fulfillment of the requirements of the degree of  
DOCTOR OF PHILOSOPHY*

to the



**INDIAN INSTITUTE OF TECHNOLOGY DELHI  
JUNE 2025**

# CERTIFICATE

It is certified that the thesis entitled “**Design, Development and Control of Battery-Solar-DFIG Based Microgrid with Synchronization to Grid,**” being submitted by **Mr. Sudip Bhattacharyya** for award of the degree of **Doctor of Philosophy** in the Department of Electrical Engineering, Indian Institute of Technology Delhi, is a record of the student work carried out by her under my supervision and guidance. The matter embodied in this thesis, has not been submitted for the award of any other degree or diploma.

**Dated:**

**(Dr. Bhim Singh)**

**Professor  
Electrical Engineering Department  
Indian Institute of Technology Delhi  
Hauz Khas, New Delhi-110016, India**

## ACKNOWLEDGMENTS

I wish to express my deepest gratitude and indebtedness to **Prof. Bhim Singh** for providing me guidance and constant supervision to carry out the Ph.D. work. Working under him has been a wonderful experience, which has provided a deep insight to the world of research. Determination, dedication, innovativeness, resourcefulness, and discipline of **Prof. Bhim Singh** have been the inspiration for me to complete this work. His consistent encouragement, continuous monitoring and commitments to excellence have always motivated me to improve my work and use the best of my capabilities. Due to his blessings, I have earned various experiences other than research, which will help me throughout my life. My sincere thanks and deep gratitude are to **Prof. Anandarup Das, Prof. B.K.Panigrahi, Prof. Santanu Mishra, Prof. Sukumar Mishra and Prof. T.C kandpal**, all SRC members for their valuable guidance and consistent support during my research work.

I wish to convey my sincere thanks to **Prof. Bhim Singh, Prof. B. P. Singh, Prof. Amit. Kumar. Jain and Prof. M. Veerachary** for their valuable inputs during my course work, which made the foundation for my research work. I am grateful to **IIT Delhi** for providing me the research facilities. I wish to express my sincere gratitude to **Prof. G. Bhuvaneswari, Prof. M. Veerachary and Prof. Anandarup Das** Prof. in-charge, PG Machine Lab., for providing me immense facilities to carry out experimental work. Thanks to Mr. Srichand, Mr. Puran Singh, and Mr. Jitendra and Mr. Anurag, of PG Machines Lab., IIT Delhi for providing me the facilities and assistance during this work. Moreover, I would like to thank the **Department of Science and Technology (DST)**, India for funding this research work under project grant number FIST Scheme (RP03195), SERI-II (RP03357) and SERB National Science Chair. I would like to thank my seniors, Dr. Ikhlq Hussain, Dr. Rajan Sonakar, Dr. Nishant Kumar, Dr. Aniket Anand, Dr. Shailendra Kumar Dwivedi, Dr. Anjaneesh Mishra, Dr. Sachin Devassy, Dr.

Saurabh Shukla, Dr. Piyush Kant for motivating me in the starting of my research work. I would like to use this opportunity to thank Dr. Nishant Kumar, Dr. Shailendra Dwivedi, Dr. Ikhlq Hussain, Dr. Anshul Varshney for providing me with valuable technical and non-technical support.

I would like to thank Mr. Sandeep Sahoo and Mr. Saran Chourasiya, Dr. Shivam Yadav and Dr. Sambasivaiah for their constant support and encouragement throughout my PhD work. I also wish to take this opportunity to thank Dr. Utkarsh Sharma, Dr. Rashmi Rai, Mrs. Yashi Singh, Dr. Vineet P Chandra, Dr. Priyank shah, Dr. Dipu Vijaya M, Dr. Shataskshi Sharma, Mrs. Aakanksha Rajput, Dr. Vivek Narayanan, Dr. Debasish Mishra, Dr. Anjeet Verma, Mr. Gurmeet Singh, Dr. Sreejith R, Dr. Radha Kushwaha, Dr. Vandana Jain, Dr. Seema Kewat, Dr. Subhra, Dr. Nidhi Mishra, Dr. Farheen Chishti, Dr. Pavitra Shukl, Ms. Sunaina Singh, Dr. Sai Pranith Girimaji, Dr. Tripurari Nath for the encouragement they have provided. I would like to thank Dr. Gaurav Modi, Mr. Bilal Naqvi, Dr. K.P. Tomar, Dr. Sunil Pandey, Dr. Shalvi Tyagi, Dr. Rohini Sharma, Ms. Chandrakala, Ms. Kousalya, Dr. Aryadip Sen, Dr. Kashif, Mr. Sharan Shastri, Dr. Hina Parveen, Dr. Yalavarthi Amarnath, Mr. Priyabrat Vats, Dr. Suri Paneeth, Dr. Jitendra Gupta, Mr. Rahul Kumar, Mr. Sayandev Ghosh, Mr. Utsav Sharma, Mr. Deepak shaw, Dr. Souvik Das, Ms. Kripa, Ms. Farha Siddique, Ms. Smita, Mr. Zarkab, Mr. Saurabh, Mr. Vipin, Mr. Rohit, Mr. Arjun, Mr. Biswajit, Mr. Sumit, Mr. Gaurav, Mr. Himanshu, and all PG Machines lab group for their valuable support. I would like to thank Dr. Dhiman Das, Dr. Debargha Brahma, who supported and inspired me during my stay in the campus. I would also like to thank Mr. Yatindra, Mr. Satish, Mr. Sandeep, and all other Electrical Engineering office staff for being supportive throughout. I am likewise thankful to those who have directly or indirectly helped me to finish my dissertation study.

I would like to thank my Mother, Mrs. Bulu Bhattacharyya, Father, Mr. Priotosh Bhattacharyya, Sister, Sudipta Chatterjee for their blessings, and constant

encouragement. I would like to thank my wife, Mrs. Arjita Bhattacharyya for giving me the inner strength and wholehearted support. I would like to thank all my respected colleagues specially Mr. Sandeep Kashyap, Dr. Sayd Naqvi, Mr. Neeraj Gupta, Mr. Manish Ahuja for their continuous support and encouragement. Their trust in my capabilities had been a key factor to all my achievements.

At last, I am beholden to Almighty for their blessings to help me to raise my academic level to this stage. I pray for their benediction in my future endeavours. Their blessings may be showered on me for strength, wisdom, and determination to achieve in future.

**Date:**

**Sudip Bhattacharyya**

# ABSTRACT

The rapid advancement of renewable energy has profoundly transformed the energy sector over the past decade. Microgrids, which integrate renewable energy sources with localized loads, offer a sustainable solution to meet the growing global energy demand while mitigating environmental impacts. Typically positioned near distribution networks, microgrids employ power converters to operate effectively in both off-grid and grid-connected modes. Progress in technology, supportive policies, and the adoption of custom power devices have enhanced the flexibility and reliability of microgrids, significantly boosting their performance. However, the inherent unpredictability of renewable energy sources introduces challenges, such as irregular power generation and complex integration with the main utility grid. Furthermore, the increasing deployment of microgrids within the power grid brings issues such as poor power factor, stability concerns, power quality degradation, and intricate power management requirements. To overcome these challenges, it is essential to develop advanced circuit configurations and sophisticated control algorithms that ensure the efficient and stable operation of microgrids. These innovations are crucial for enabling a sustainable and resilient energy future.

This research emphasizes the development of a variable-speed, fixed-pitch wind energy generation system (WEGS) designed with doubly fed induction generator (DFIG) for efficient energy utilization. The system features two voltage source converters (VSCs) arranged in a back-to-back configuration with a shared DC link. The rotor-side converter (RSC) is responsible for maximizing wind energy extraction, while the grid-side converter (GSC) ensures smooth integration with the utility grid, managing power flow to the grid and local loads, including auxiliary services. For solar energy generation, the system can be designed to operate in either single-stage or two-stage configurations, depending on the

specific application requirements. The primary objective is to achieve efficient energy generation from both variable-speed wind turbines and solar photovoltaic arrays. Key challenges include maintaining consistent power output despite fluctuations in wind speed and solar irradiance, as well as ensuring stable and reliable grid integration.

This study explores two distinct configurations for forming a local grid. The first configuration employs a grid-forming converter (GFC) supported by a photovoltaic (PV) array and a battery energy storage system (BESS). The second configuration utilizes a GFC exclusively powered by a BESS. In the PV-based system, maximum power extraction is achieved through the incremental conductance (INC) algorithm, while the wind-driven doubly-fed induction generator (DFIG) uses a maximum power point tracking (MPPT) algorithm to optimize wind energy capture. The stator windings of the DFIG are synchronized with the local grid to ensure seamless integration. To maintain efficient microgrid operation, a robust control algorithm is essential. This research introduces an advanced control strategy designed to ensure smooth microgrid performance under dynamic conditions, including load connection and disconnection, variations in wind speed, and changes in solar insolation. The proposed approach enhances the reliability and stability of the microgrid, even in fluctuating environmental and operational scenarios.

The microgrid architecture and control strategies are initially validated through software simulations using the MATLAB/Simulink platform. Following promising results, a physical prototype of a microgrid is constructed, incorporating a wind turbine driven doubly-fed induction generation (DFIG), a solar photovoltaic array, and a battery energy storage system (BESS). This prototype is subjected to extensive testing across various configurations, utilizing appropriate control algorithms to evaluate performance.

The simulated and experimental results are analyzed under a range of challenging conditions, including fluctuations in wind speed, solar insolation, unbalanced and balanced

loads. Notably, the system demonstrates effective maximum power point tracking (MPPT) for wind and solar energy under normal conditions. Additionally, the microgrid's performance is assessed during both off-grid and grid-interactive operations, showcasing a smooth transition between these modes. The results highlight the capability of this multi-functional microgrid to maintain reliability and efficiency under diverse operational scenarios.

नवीकरणीय ऊर्जा की तीव्र प्रगति ने पिछले दशक में ऊर्जा क्षेत्र को गहराई से बदल दिया है। माइक्रोग्रिड, जो स्थानीय भार के साथ नवीकरणीय ऊर्जा स्रोतों को एकीकृत करता है, पर्यावरणीय प्रभावों को कम करते हुए बढ़ती वैश्विक ऊर्जा मांग को पूरा करने के लिए एक स्थायी समाधान प्रदान करता है। आमतौर पर वितरण नेटवर्क के पास स्थित, माइक्रोग्रिड ऑफ-ग्रिड और ग्रिड-कनेक्टेड दोनों मोड में प्रभावी ढंग से काम करने के लिए पावर कन्वर्टर्स का उपयोग करते हैं। प्रौद्योगिकी में प्रगति, सहायक नीतियों और कस्टम बिजली उपकरणों को अपनाने से माइक्रोग्रिड के लचीलेपन और विश्वसनीयता में वृद्धि हुई है, जिससे उनके प्रदर्शन में काफी वृद्धि हुई है। हालाँकि, नवीकरणीय ऊर्जा स्रोतों की अंतर्निहित अप्रत्याशितता अनियमित बिजली उत्पादन और मुख्य उपयोगिता ग्रिड के साथ जटिल एकीकरण जैसी चुनौतियाँ पेश करती है। इसके अलावा, पावर ग्रिड के भीतर माइक्रोग्रिड की बढ़ती तैनाती खराब बिजली कारक, स्थिरता संबंधी चिंताएं, बिजली की गुणवत्ता में गिरावट और जटिल बिजली प्रबंधन आवश्यकताओं जैसे मुद्दे लाती है। इन चुनौतियों से पार पाने के लिए, उन्नत सर्किट कॉन्फ़िगरेशन और परिष्कृत नियंत्रण एल्गोरिदम विकसित करना आवश्यक है जो माइक्रोग्रिड के कुशल और स्थिर संचालन को सुनिश्चित करते हैं। टिकाऊ और लचीले ऊर्जा भविष्य को सक्षम करने के लिए ये नवाचार महत्वपूर्ण हैं।

यह शोध कुशल ऊर्जा उपयोग के लिए डिज़ाइन की गई एक चर-गति, निश्चित-पिच पवन ऊर्जा उत्पादन प्रणाली (WEGS) के विकास पर जोर देता है। सिस्टम में दो वोल्टेज स्रोत कनवर्टर (वीएससी) हैं जो एक साइड डीसी लिंक के साथ बैक-टू-बैक कॉन्फ़िगरेशन में व्यवस्थित हैं। रोटर-साइड कनवर्टर (आरएससी) पवन ऊर्जा निष्कर्षण को अधिकतम करने के लिए जिम्मेदार है, जबकि ग्रिड-साइड कनवर्टर (जीएससी) उपयोगिता ग्रिड के साथ सुचारु एकीकरण सुनिश्चित करता है, सहायक सेवाओं सहित ग्रिड और स्थानीय

भार में बिजली के प्रवाह का प्रबंधन करता है। सौर ऊर्जा उत्पादन के लिए, सिस्टम को विशिष्ट अनुप्रयोग आवश्यकताओं के आधार पर एकल-चरण या दो-चरण कॉन्फिगरेशन में संचालित करने के लिए डिज़ाइन किया जा सकता है। प्राथमिक उद्देश्य चर-गति पवन टर्बाइन और सौर फोटोवोल्टिक सरणियों दोनों से कुशल ऊर्जा उत्पादन प्राप्त करना है। प्रमुख चुनौतियों में हवा की गति और सौर विकिरण में उतार-चढ़ाव के बावजूद लगातार बिजली उत्पादन बनाए रखना, साथ ही स्थिर और विश्वसनीय ग्रिड एकीकरण सुनिश्चित करना शामिल है।

यह अध्ययन स्थानीय ग्रिड बनाने के लिए दो अलग-अलग कॉन्फिगरेशन की खोज करता है। पहला कॉन्फिगरेशन एक फोटोवोल्टिक (पीवी) सरणी और एक बैटरी ऊर्जा भंडारण प्रणाली (बीईएसएस) द्वारा समर्थित ग्रिड-फॉर्मिंग कनवर्टर (जीएफसी) को नियोजित करता है। दूसरा कॉन्फिगरेशन विशेष रूप से BESS द्वारा संचालित GFC का उपयोग करता है। पीवी-आधारित प्रणाली में, अधिकतम बिजली निष्कर्षण वृद्धिशील संचालन (आईएनसी) एल्गोरिदम के माध्यम से प्राप्त किया जाता है, जबकि पवन-चालित डबल-फेड इंडक्शन जनरेटर (डीएफआईजी) टिप-स्पीड अनुपात-आधारित अधिकतम पावर पॉइंट ट्रैकिंग (एमपीपीटी) एल्गोरिदम का उपयोग करता है। पवन ऊर्जा कैप्चर को अनुकूलित करने के लिए। निर्बाध एकीकरण सुनिश्चित करने के लिए डीएफआईजी की स्टेटर वाइंडिंग्स को स्थानीय ग्रिड के साथ सिंक्रनाइज़ किया गया है। कुशल माइक्रोग्रिड संचालन को बनाए रखने के लिए, एक मजबूत नियंत्रण एल्गोरिदम आवश्यक है। यह शोध एक उन्नत नियंत्रण रणनीति पेश करता है जो गतिशील परिस्थितियों में सुचारु माइक्रोग्रिड प्रदर्शन सुनिश्चित करने के लिए डिज़ाइन की गई है, जिसमें लोड कनेक्शन और डिस्कनेक्शन, हवा की गति में बदलाव और सौर सूर्यातप में परिवर्तन शामिल हैं। प्रस्तावित दृष्टिकोण उतार-चढ़ाव वाले पर्यावरणीय और परिचालन परिदृश्यों में भी माइक्रोग्रिड की विश्वसनीयता और स्थिरता को बढ़ाता है।

माइक्रोग्रिड आर्किटेक्चर और नियंत्रण रणनीतियों को प्रारंभ में MATLAB/Simulink प्लेटफॉर्म का उपयोग करके सॉफ्टवेयर सिमुलेशन के माध्यम से मान्य किया जाता है। आशाजनक परिणामों के बाद, एक माइक्रोग्रिड का एक भौतिक प्रोटोटाइप बनाया गया है, जिसमें एक पवन चालित डबल-फेड इंडक्शन जेनरेशन (डीएफआईजी), एक सौर फोटोवोल्टिक सरणी और एक बैटरी ऊर्जा भंडारण प्रणाली (बीईएसएस) शामिल है। प्रदर्शन का मूल्यांकन करने के लिए उपयुक्त नियंत्रण एल्गोरिदम का उपयोग करते हुए, इस प्रोटोटाइप को विभिन्न कॉन्फिगरेशन में व्यापक परीक्षण के अधीन किया गया है।

सिम्युलेटेड और प्रयोगात्मक परिणामों का विश्लेषण कई चुनौतीपूर्ण परिस्थितियों में किया जाता है, जिसमें हवा की गति और सौर सूर्यातप में उतार-चढ़ाव, असंतुलित और संतुलित भार शामिल हैं। विशेष रूप से, सिस्टम सामान्य परिस्थितियों में पवन और सौर ऊर्जा के लिए प्रभावी अधिकतम पावर प्वाइंट ट्रैकिंग (एमपीपीटी) प्रदर्शित करता है। इसके अतिरिक्त, ऑफ-ग्रिड और ग्रिड-इंटरैक्टिव संचालन दोनों के दौरान माइक्रोग्रिड के प्रदर्शन का मूल्यांकन किया जाता है, जो इन मोडों के बीच एक सहज संक्रमण को दर्शाता है। परिणाम विविध परिचालन परिदृश्यों के तहत विश्वसनीयता और दक्षता बनाए रखने के लिए इस बहु-कार्यात्मक माइक्रोग्रिड की क्षमता को उजागर करते हैं।

# TABLE OF CONTENTS

Certificate	i
Acknowledgments	ii
Abstract	v
Table of Contents	xi
List of Figures	xviii
List of Tables	xxi
List of Abbreviations	xxii
List of Symbols	xxiv

## CHAPTER I INTRODUCTION

1.1	General	1
1.2	State of Art	4
1.2.1	Wind Driven DFIG-PV-Battery Based System for Islanded and Re-synchronizable Mode of Operation	4
1.2.2	MPPT Techniques for Wind Turbine and Solar PV Array	5
1.2.3	Control Algorithms for Wind Driven DFIG-PV-Battery Based Grid-Synchronized System	6
1.2.4	Power Quality Improvement in Microgrid	8
1.3	Scope of Work	8
1.4	Outline of Chapters	9

## CHAPTER II LITERATURE REVIEW

2.1	General	12
2.2	Literature Survey	13
2.2.1	Review Battery Energy Storage	13
2.2.2	Review of Single and Double Stage PV Array	14
2.2.3	Review Wind Driven DFIG and Its Controls	16
2.2.3.1	Control Strategies of DFIG	16
2.2.4	Review of Hybrid Microgrid and Its Controls	19
2.3	Identified Research Areas	20
2.4	Conclusions	20

## CHAPTER III DESIGN AND CONTROL OF STANDALONE PV-BATTERY BASED MICROGRID WITH SYNCHRONIZATION OF WIND DRIVEN DOUBELY-FED INDUCTION GENERATOR

3.1	General	22
3.2	System Configuration of Standalone Microgrid with Integration of Battery PV and DFIG	23

3.3	Design and Selection of Parameters for Standalone Microgrid	24
3.3.1	Selection of PV Array	24
3.3.2	Design and Selection of Solar PV Array Link Capacitor	25
3.3.3	Design and Selection of Inductor in DC-DC Boost Converter	26
3.3.4	Design and Selection of DC Link Capacitor	26
3.3.5	Design and Selection of Interfacing Inductor of PV Battery VSC	27
3.3.6	Design and Selection of Ripple Filter	28
3.3.7	Selection of IGBT Module for Voltage Source Converter	28
3.4	Selection And Modeling of DFIG Based Wind Turbine	29
3.4.1	Model of Wind Turbine	29
3.5	Control Technique	31
3.5.1	Incremental Conductance Based MPPT Technique for PV Array	31
3.5.2	Control of Grid Forming Converter	33
3.5.3	RSC Control for DFIG	34
3.5.4	Grid Side Converter Control	38
3.6	MATLAB Simulation Model for Standalone Microgrid	41
3.7	Hardware Implementation	42
3.8	Results and Discussion	46
3.8.1	Simulated Performances	46
3.8.1.1	Performance of Battery and PV Based GFC at Solar Dynamic Variation	46
3.8.1.2	Performance of DFIG at Stator Windings Synchronization	48
3.8.1.3	Performance of Wind Turbine and DFIG at Wind Speed Variations	48
3.8.1.4	Internal Signals of GSC at Load Connection and Disconnection	49
3.8.1.5	Performance of RSC and Its Internal Signals at Wind Speed Variations	50
3.8.1.6	Harmonics Analysis and Comparison Study of Proposed Hybrid Microgrid	51
3.8.2	Experimental Performances	52
3.8.2.1	Performance of DFIG at Different Wind Speeds and Load Dynamic Variants	53
3.8.2.2	Intermediate Signals Response of DFOGI-FLL Controller	54
3.8.2.3	Performance of DFIG at Stator Synchronization	55
3.8.2.4	Performance of PV and Battery with GFC	55
3.9	Conclusions	58

**CHAPTER IV DESIGN AND CONTROL OF STANDALONE BATTERY WITH BDC PV BASED MICROGRID WITH SYNCHRONIZATION OF WIND DRIVEN DOUBELY-FED INDUCTION GENERATOR**

4.1	General	59
4.2	Configuration of PV-Battery with BDC Based GFC with Integration of DFIG	60
4.3	Design and Selected Parameters of Control Battery, PV and DFIG Based Standalone Microgrid	61
4.4	Selection and Modeling of Wind Driven DFIG	62
4.5	Control Technique	62
4.5.1	Grid Forming Converter Control Algorithm	62
4.5.2	BDC Based Battery Control Algorithm	64
4.5.3	TDSOGI-FLL-WPF Based GSC Control	65
4.5.4	Rotor Side Converter Control	68
4.6	MATLAB Simulation of Battery Based GFC With Integration of PV and DFIG	72
4.7	Hardware Implementation	73
4.8	Results and Discussion	73
4.8.1	Simulated Performances	73
4.8.1.1	Performance of Battery PV based GFC with Different Solar Insolation	73
4.8.1.2	Stator Windings Synchronization of DFIG with Local Grid	73
4.8.1.3	Performance of Wind Turbine at Different Wind Speed	75
4.8.1.4	Performance of DFIG at Different Wind Speed	76
4.8.1.5	Performance of Microgrid at Different Wind Speed	78
4.8.1.6	Harmonics Analysis and Comparison Study of Proposed Hybrid Microgrid	79
4.8.2	Experimental Performances	79
4.8.2.1	Performance of PV with Varying Insolation	80
4.8.2.2	Dynamic Effect on Battery-PV at Load disconnection, Load Connection and Varying Solar Insolation	80
4.8.2.3	Dynamic Effect on Battery-PV at Different Wind Speeds and Varying Solar Insolation	82
4.8.2.4	Performance of DFIG Before and during Stator Synchronization	82
4.8.2.5	Internal RSC Signals After Stator Synchronization	83
4.9	Conclusions	84

**CHAPTER V DESIGN AND CONTROL OF STANDALONE BATTERY BASED GRID FORMING CONVERTER WITH PV AND SYNCHRONIZATION OF WIND DRIVEN DOUBELY-FED INDUCTION GENERATOR**

5.1	General	85
5.2	System Configuration of Wind Driven DFIG Integration with Battery Based GFC and PV	86
5.3	Design and Selected Parameters of Battery, PV and DFIG Based Standalone Microgrid	87
5.4	Selection and Modeling of Wind Driven DFIG	88
5.5	Control Technique	88
5.5.1	Grid Forming Converter Control Technique	88
5.5.2	PV-VSC Control Algorithm	90
5.5.3	Advanced Three Phase Comb FLL Control for GSC	92
5.5.4	Rotor Side Converter Control	96
5.6	Simulated Performance of DFIG With Integration of Battery Based GFC and PV	100
5.7	Hardware Implementation	101
5.8	Results and Discussion	101
5.8.1	Simulated Performances	101
5.8.1.1	Dynamic Performance of PV-Battery at Different Load and Solar Insolation	101
5.8.1.2	Performance of Battery-PV Microgrid at Different Load	102
5.8.1.3	Performance of GSC at Load Variations	102
5.8.1.4	Performance of RSC at Wind Speed Variations	103
5.8.1.5	Operation of Stator Synchronization	104
5.8.1.6	Power Variation at Different Dynamic Conditions	104
5.8.2	Experimental Performances	105
5.8.2.1	Performance of Battery with Load variation	106
5.8.2.2	Performance of PV at Different Solar Insolation and Internal Signals of PV-VSC	106
5.8.2.3	Performance of GSC and RSC at Different Wind Speed and Load Variation	107
5.8.2.4	Internal Signals of GSC	109
5.8.2.5	Internal Signals of RSC	109
5.8.2.6	Voltage Developed in GFC and Stator Windings of DFIG	110
5.8.2.7	Stator Windings Synchronization with PCC	110
5.9	Conclusions	111

**CHAPTER VI DESIGN AND CONTROL OF 3P4W STANDALONE BATTERY BASED GRID FORMING CONVERTER WITH PV AND SYNCHRONIZATION OF WIND DRIVEN DOUBELY-FED**

## INDUCTION GENERATOR

6.1	General	112
6.2	System Configuration of Hybrid PV Wind and Battery Based Microgrid	113
6.3	Design and Selected Parameters of Battery, PV and DFIG Based Standalone Microgrid	113
6.4	Selection and Modeling of Wind Driven DFIG	115
6.5	Control Technique	115
6.5.1	Control Algorithm for GFC	115
6.5.2	Comb Sliding Mode Based GSC Control	116
6.5.3	Control Algorithm for RSC of DFIG	119
6.5.4	Control Algorithm for PV based VSC	123
6.6	MATLAB Simulation of Battery Based GFC With Integration of PV and DFIG	125
6.7	Hardware Implementation	126
6.8	Results and Discussion	126
6.8.1	Simulated Performances	126
6.8.1.1	Performance of Wind Turbine at Different Wind Speed	126
6.8.1.2	Dynamic Performance of Battery, PV and DFIG	126
6.8.1.3	Performance of GSC at Load Disconnection and Connection	128
6.8.1.4	Performance of Battery at Different Solar Insolation	129
6.8.1.5	Performance of Battery at DFIG Stator Synchronization	130
6.8.1.6	Harmonics Analysis	131
6.8.2	Experimental Performances	132
6.8.2.1	Operation of DFIG at Wind and Load Dynamic Conditions	132
6.8.2.2	Intermediate Signals of GSC and RSC at Load Variation and at Steady-State	133
6.8.2.3	GSC Internal Signals at Load Variation and at Steady-State	134
6.8.2.4	Performance of Load Neutral Current Compensation	135
6.8.2.5	Performance of PV Array and PV Based Converter Control	136
6.9	Conclusions	137

## **CHAPTER VII DESIGN AND CONTROL OF BATTERY BASED GRID FORMING CONVERTER, PV AND WIND DRIVEN DOUBELY-FED INDUCTION GENERATOR WITH GRID SYNCHRONIZATION**

7.1	General	138
7.2	Configuration of Grid-Connected Hybrid PV, Wind and Battery Based Microgrid	139
7.3	Design and Selected of Parameters of Battery, PV Array and DFIG Based Microgrid	139

7.4	Selection and Modeling of Wind Driven DFIG	141
7.5	Control Technique	141
7.5.1	Control Algorithm for Battery Based GFC	141
7.5.2	CBPF-FLL Based Grid Following Control	143
7.5.3	RSC Control Before Stator Windings Synchronization	146
7.5.4	RSC Control After Stator Windings Synchronization	148
7.5.5	Control Algorithm for PV Array based VSC	150
7.6	MATLAB Simulation of Islanded and Grid Mode Operation of Battery Based GFC with Integration of Wind And PV	153
7.7	Hardware Implementation	154
7.8	Results and Discussion	154
7.8.1	Simulated Performances	154
7.8.1.1	Performance of Battery Based Converter Before and After Grid Synchronization	154
7.8.1.2	DFIG Stator Windings Synchronization	155
7.8.1.3	Dynamic Performance of RSC	155
7.8.1.4	Performance of PV Array at Different Solar Insolation	155
7.8.1.5	Harmonics Analysis	158
7.8.2	Experimental Performances	158
7.8.2.1	Battery Assisted GFC Operation	159
7.8.2.2	Operation of DFIG at Dynamic Speed Variation	160
7.8.2.3	Performance of GSC at Load and Wind Dynamics	161
7.8.2.4	Performance of PV at Dynamic Solar Irradiance	161
7.8.2.5	Stator Windings Synchronization of DFIG Using CBP-FLL	162
7.8.2.6	Standalone to Grid Mode of Operation	163
7.8.2.7	Operation of Power Balancing at Different Dynamics	164
7.9	Conclusions	165

## **CHAPTER VIII MAIN CONCLUSIONS AND SUGGESTIONS FOR FURTHER WORK**

8.1	General	166
8.2	Main Conclusions	167
8.3	Suggestion for Further Work	170
	<b>REFERENCES</b>	172
	<b>LIST OF PUBLICATIONS</b>	180
	<b>BIODATA</b>	183

## LIST OF FIGURES

Fig. 3.1	Schematic diagram of hybrid battery wind and PV based microgrid
Fig. 3.2	INC based MPPT algorithm for solar PV array
Fig. 3.3	Control algorithm for battery-PV supported GFC
Fig. 3.4	RSC control for DFIG
Fig. 3.5	GSC of the DFIG
Fig. 3.6	DFOGI-FLL linearized model of phase <i>a</i> load current
Fig. 3.7	DFOGI-FLL linearized model of DFIG angle
Fig. 3.8	Bode plot for DFOGI-FLL linearized model
Fig. 3.9	MATLAB Simulink model for hybrid PV, BESS and DFIG based standalone system
Fig. 3.10	Schematic diagram of LEM LV 25P
Fig. 3.11	PCB of LEM LV 25P voltage sensor board
Fig. 3.12	Schematic diagram LEM LA 55P
Fig. 3.13	PCB of LEM LA 55P current sensor board
Fig. 3.14	Schematic diagram opto-coupler
Fig. 3.15	PCB of opto-coupler board
Fig. 3.16	Hardware setup for hybrid PV-wind battery based microgrid
Fig. 3.17	Performance of battery-PV based grid forming converter
Fig. 3.18	Performance of DFIG stator synchronization to local grid
Fig. 3.19	Performance of turbine parameters at wind speed variation
Fig. 3.20	GSC internal signals at disconnection and connection of load
Fig. 3.21	Performance RSC at speed variation
Figs. 3.22 (a)-(b)	Harmonic spectrum of standalone grid voltage
Figs. 3.23 (a)-(b)	Harmonic spectrum of stator Current
Fig. 3.24	Comparison With State-of Art Between Improved DFOGI and Others Controller
Figs. 3.25 (a)-(f)	Dynamic variation of DFIG at different wind speed and load
Fig. 3.26 (a)-(b)	Internal responses of DFOGI-FLL controller
Figs. 3.27 (a)-(b)	Performance of the DFIG during stator synchronization
Figs. 3.28 (a)-(k)	Performance of the DFIG during stator synchronization
Fig. 4.1	Schematic of PV battery based GFC with integration of DFIG
Fig. 4.2	PV-battery with grid forming converter
Fig. 4.3	PI based battery control technique
Fig. 4.4	TDSOGI-FLL-WPF control for GSC of DFIG
Fig. 4.5	Bode plot of load current component at different range of parameters
Figs. 4.6 (a)-(b)	RSC control before and after stator synchronization
Fig. 4.7	MATLAB Simulink model for hybrid PV, BESS and DFIG based standalone system
Fig. 4.8	Performance of battery-PV based grid forming converter
Fig. 4.9	Performance of DFIG stator synchronization to local grid
Fig. 4.10	Performance of wind turbine at speed change
Fig. 4.11	Performance of doubly fed induction generator at different wind speed
Fig. 4.12	Performance of microgrid at different wind speed and solar irradiances
Figs. 4.13 (a)-(b)	Harmonic spectrum of standalone grid voltage
Figs. 4.14 (a)-(b)	Harmonic spectrum of stator Current
Fig. 4.15	Solar power variations at different insolation

Figs. 4.16(a)-(c)	Dynamic analysis of PV and battery due to load variation
Fig. 4.17	Dynamic analysis of PV and battery due to wind and solar variation
Figs. 4.18(a)-(c)	Performance during DFIG stator synchronization
Fig. 4.19	Internal RSC signal after stator winding synchronization
Fig. 5.1	Battery-PV-DFIG based microgrid
Fig. 5.2	Grid forming converter control
Fig. 5.3	PV-VSC control algorithm
Fig. 5.4	Comb-FLL control for GSC of machine
Figs. 5.5 (a)-(b)	RSC control before and after stator synchronization
Fig. 5.6	MATLAB Simulink model for hybrid PV, BESS and DFIG based standalone system
Fig. 5.7	Performance of battery-PV and load at different solar insolation
Fig. 5.8	Performance of battery-PV at load variation
Fig. 5.9	Performance of GSC with Comb-FLL
Fig. 5.10	Performance of RSC at varying wind speed
Fig. 5.11	Performance of DFIG at stator synchronization
Fig. 5.12	Power variation of microgrid due to dynamics
Figs. 5.13 (a)-(b)	Battery dynamics at load variation
Figs. 5.14 (a)-(c)	Operation of PV at different insolation
Figs. 5.15 (a)-(g)	Dynamic performance of GSC and RSC
Figs. 5.16 (a)-(b)	Intermediate signals of GSC control
Fig. 5.17	Intermediate signals of RSC control
Figs. 5.18 (a)-(b)	Intermediate signals of RSC control at varying wind speed
Fig. 5.19	Stator windings synchronization with PCC
Fig. 6.1	DFIG-battery-PV based 3P4W system configuration
Fig. 6.2	Control scheme for battery-based grid forming converter
Fig. 6.3	CSM based control scheme for GSC
Figs. 6.4 (a)-(b)	Control scheme for stator synchronization and control of RSC
Fig. 6.5	Control scheme for PV-VSC
Fig. 6.6	MATLAB Simulink model for battery based GFC with PV and DFIG integration
Fig. 6.7	Operation of WT and DFIG at various wind
Fig. 6.8	Battery, PV and DFIG Performance at solar, wind and load dynamics
Fig. 6.9	Performance of GSC control under load dynamics
Fig. 6.10	Performance of battery at different solar irradiance
Fig. 6.11	Performance of battery at DFIG stator synchronization
Figs. 6.12 (a)-(b)	Harmonic spectrum of standalone grid voltage
Figs. 6.13 (a)-(b)	Harmonic spectrum of stator Current
Figs.6.14 (a)-(c)	Performance of the microgrid under wind speed variation and load disconnection and connection
Figs.6.15 (a)-(c)	Performance of the GSC at steady-state, load disconnection and load connection condition
Figs.6.16 (a)-(c)	Stator synchronization to CCP
Figs.6.17 (a)-(c)	Performance of load neutral and converter neutral at steady-state and dynamics
Figs.6.18 (a)-(b)	Performance of PV array and PV based VSC at various solar irradiance
Fig. 7.1	Schematic of battery-DFIG-PV based microgrid
Figs. 7.2 (a)-(b)	Islanded and grid mode control of battery based VSC (a) Islanded

	mode of control, (b) Grid Connected mode of control
Fig. 7.3	Nyquist diagram of CBPF current controller
Fig. 7.4	RSC control before stator synchronization
Fig.7.5	RSC control after stator synchronization
Fig. 7.6	PV-VSC and INC MPPT control strategy
Fig. 7.7	MATLAB Simulink model for battery based GFC with PV and DFIG integration
Fig. 7.8	Performance of battery-PV based grid forming converter
Fig. 7.9	Performance of DFIG stator synchronization to local grid
Fig. 7.10	Performance of RSC
Fig. 7.11	Performance of PV-VSC at different solar insolation
Fig. 7.12	Harmonic spectrum of standalone grid voltage ( $V_{pcc}$ )
Fig. 7.13	Harmonic spectrum of stator Current
Fig. 7.14	Harmonic spectrum of grid current THD
Figs.7.15. (a)-(c)	Battery performance at dynamic load variation
Figs.7.16. (a)-(e)	Dynamic performance of DFIG at speed variation
Figs. 7.17 (a)-(b)	DFIG performance during the wind and load variation
Figs.7.18. (a)-(c)	Performance of PV at different insolation
Figs. 7.19 (a)-(c)	Synchronization of stator windings of the DFIG
Figs. 7.20 (a)-(c)	Standalone to grid mode of operation
Figs. 7.21 (a)-(b)	Battery, DFIG, load and PV power variations

## LIST OF TABLES

Table 3.1	Parameters of Wind Turbine
Table 3.2	Performance Analysis Among DFOGI-FLL and State-of-Art Method
Table 4.1	Control Parameters of RSC
Table 5.1	Pros and Cons of Comb-FLL Control with Others Advanced Controls
Table 5.2	Control Parameters of RSC
Table 6.1	Control Parameters of Battery Based Grid Forming Converter
Table 6.2	Comparison Study of Different Controller for GSC
Table 6.3	Control Parameters of GSC
Table 6.4	Control Parameters of RSC
Table 6.5	Parameters of PV-VSC Control
Table 7.1	Control Parameters of Battery Based GFC
Table 7.2	Control Parameters of RSC
Table 7.3	Parameters of RSC Stage 2 Control
Table 7.4	Parameters of PV-VSC Control

## LIST OF ABBREVIATIONS

3P3W	Three-Phase Three Wire
3P4W	Three-Phase Four Wire
AC	Alternating Current
AMAF	Adaptive Moving Average Filter
ANN	Artificial Neural Networks
ASVF	Advance Space Vector Filter
BBF	Butter Worth Band Pass Filter
BESS	Battery Energy Storage System
BDC	Bidirectional DC-DC Converter
CBPF-FLL	Complex Band-Pass Filter-Based Frequency-Locked Loop
CBPF-FLL	Complex Band Pass Filter-Based FLL
CC-ROGI	Complex Coefficient Reduced Ordered Generalised Integrator
CCP	Common Coupling Point
CMS	Comb Sliding Mode
CSM	Comb Sliding Mode
DC	Direct Current
DFIG	Doubly Fed Induction Generation
DFOGI-FLL	Discrete Fourth Order Generalized Integrator-Frequency Locked Loop
DFOGI-FLL	Double Frequency Oscillator Generalized Integrator-Frequency Locked Loop
DoD	Depth Of Discharge
DSOGI	Double Second-Order Generalized Integrator
dSpace	Digital Signal Processing And Control Engineering
DSTATCOM	Distribution Static Synchronous Compensator
ESS	Energy Storage System
EV	Electric Vehicle
FLC	Fuzzy Logic Controller
FOC	Flux-Oriented Control
FOGI	Fourth Order Generalized Integrator
GFC	Grid Forming Converter
GSC	Grid-Side Converter
GW	Gigawatts
HOGI	High-Order Generalized Integral
IEEE	Institute Of Electrical and Electronics Engineers
IGBT	Insulated Gate Bipolar Transistors
ILC	Inter-Linking Converter
IMRF	Improved Multiple Reference Frame
INC	Incremental Conductance
IRPT	Instantaneous Reactive Power Theory
ITOGI	Improved Third Order Generalized Integrator
KE	Kinetic Energy
KF	Kalman Filter
LFP	Lithium Ferro Phosphate
LG	Local Grid
LMF	Least Mean Fourth
LMS	Least Mean Square

LVRT	Low Voltage Ride Through
MATLAB	Matrix Laboratory
MPC	Model Predictive Control
MPPT	Maximum Power Point Tracking
MS-TOGI	Second- And Third-Order Generalized Integrator
OC	Orthogonal Component
P&O	Perturbation And Observation
PCB	Printed Circuit Board
PCC	Point Of Coupling
PI	Proportional-Integral
PLL	Phase Locked Loop
PPA	Power Purchase Agreement
PQ	Power Quality
PSF	Power Signal Feedback
PV	Photovoltaic
PWM	Pulse Width Modulation
ROGI	Reduced Ordered Generalized Integrator
RSC	Rotor-Side Converter
SOC	State Of Charge
SOGI	Second-Order Generalized Integrator
SOSF-FLL	Second Order Sequence Filter-Frequency Locked Loop
SRF	Synchronous Reference Frame
STS	Static Transition Switch
TDSOGI-FLL-WPF	Tustin Discretized Second Order Generalized Integrator-Frequency Locked Loop
THD	Total Harmonic Distortion
TOGI	Third-Order Generalized Integrator
TSR	Tip To Speed Ratio
VOC	Voltage Oriented Control
VSC	Voltage Source Converter
WECS	Wind Energy Conversion System
WT	Wind Turbine

## LIST OF SYMBOLS

$\theta_s$	FLL stator angle
$a$	Overloading factor
$b_1$	Energy variation is considered during dynamic change
$c, b, k_a, k_b$	Linearized controller gain
$C_{bat}$	DC-link capacitor across battery based converter
$C_{dc1}$	Capacitor of PV-VSC
$C_{dc2}$	Capacitor of GSC
$C_f$	Capacitance of the ripple filter
$C_p$	Power coefficient
$C_{pmax}$	Maximum theoretical value of power coefficient
$c_{pv}$	Capacitor across PV array
$D$	Duty cycle
$E_b$	Battery voltage
$e_{idr}$	Error between reference and actual rotor $d$ -axis current
$e_{rdgr}$	Error between stator and PCC terminal voltage
$e_{rdgr}$	Error ( $e_{rdgr}$ ) between stator and CCP terminal voltage
$e_{riqr}$	Difference of reference and actual $q$ -axis current
$e_{rqs}$	Difference between reference and actual reactive power $Q_s$
$err_{dpv}, err_{qpv}$	$D$ -axis and $q$ -axis error voltage of GFC control
$er_\theta$	Error component between stator and PCC angle
$er_{\omega m}$	Error between reference and actual rotor speed
$f$	Line frequency
$f_{ccp}$	Line frequency at CCP
$F_s$	Stator flux of DFIG
$f_s$	Switching frequency
$F_s$	Stator flux
$G_1, G_2$	Adaptive gains
$I_{am}, I_{bm}, I_{cm}$	Active load current component
$I_{bat}$	Battery current
$I_{bater}$	Difference between the reference current and actual battery current
$I_{batre}$	Reference battery current
$I_{bc}$	Battery charging current
$I_{bd}$	Battery discharging current
$i_c$	Sensed converter currents
$i_{ca}, i_{cb}$ and $i_{cc}$	Three phase converter currents (PV-VSC)
$i_{caf}, i_{cbf}, i_{cef}$	Three phase Reference GFC currents
$I_{cdf}, I_{caf}$	$D$ -axis and $Q$ -axis current of GFC
$i_{cer}$	Error signals of GFC current
$I_{cmax}$	Maximum current of the VSC
$I_{cmax, peak}$	Maximum peak current of the VSC
$i_{cref}$	Reference converter current
$i_d$	Load current in $d$ -axis
$I_{dbat}, I_{qbat}$	Converter reference currents
$i_{dfig}$	DFIG currents (combination of GSC and stator current)
$I_{dr}$	Actual rotor $d$ -axis current
$I_{dr1}$	Internal $d$ -axis rotor current
$I_{dref}$	$D$ -axis rotor reference current, first part of RSC control

$I_{drref}$	$D$ -axis reference rotor current
$I_{Drt}, I_{Qrt}$	$D$ -axis and $Q$ -axis rotor currents component
$i_{err}$	Error between reference and actual PCC current
$i_{gabc}$	Grid current
$i_{gref}$	Reference PCC current
$i_{gsc}$	GSC currents
$I_{IGBT}$	IGBT current
$i_L$	Load current
$i_{La}, i_{Lb}$ and $i_{Lc}$	Three phase load currents
$i_{Lad}$	In-phase load current components
$i_{Laq}$	Load current components
$I_{Lav}$	Average load current component
$I_{Line}$	Line current
$i_{Lma}, i_{Lmb}, i_{Lmc}$	Active load component in phase- $abc$
$I_{loss2}$	Loss current component
$I_{mppv}$	Maximum MPPT current
$i_p$	Primary current
$I_{pav}$	Average current component
$I_{pnet}$	Net active current component
$I_{pnet}$	Net active component
$I_{pv}$	PV current
$I_{qr1}$	Internal $q$ -axis rotor current
$I_{qref}$	$Q$ -axis rotor reference current, first part of RSC control
$I_{qref}$	Reference $q$ -axis RSC current
$i_r$	Rotor current
$i_{raf}, i_{rbf}, i_{rcf}$	Three phase reference rotor currents in first part of RSC control
$i_{rerr}$	Error between reference and actual rotor current
$i_{rsc}$	RSC currents
$i_s$	Secondary current
$i_{sa}, i_{sb}$ and $i_{sc}$	Stator currents
$i_{sabc}$	Actual CCP/PCC current
$I_{sca}$	Short circuit current
$i_{sense}$	Current input to the sensor
$i_{a1}, i''_{a1}, i_{\beta1}$ and $i''_{\beta1}$	Internal signals of CBPF-FLL control
$i_{of1}$ and $i_{\beta1}$	Filter load current components
$k$	Constant gain
$k_a$ and $k_b$	Forward path gain
$k_g$	Accelerate or decelerate the process
$k_i$	Integral gain
$k_p$	Proportional gain
$k_{p1}, k_{p2}, k_{i1}, k_{i2}$	PI controller gain for GFC control
$k_{pd}, k_{id}, k_{i\theta}$	PI controller gain of RSC control before stator windings synchronization
$k_{pdgi}, k_{idgi}$	PI controller gain of GSC control
$k_{pr1}, k_{ir1}, k_{pr2}, k_{ir2},$ $k_{p\omega1}, k_{i\omega1}, k_{p\omega2}, k_{i\omega2}$	PI controller gain of RSC control after stator windings synchronization
$L$	Inductor of DC-DC converter
$L_b$	Inductor of DC-DC converter
$L_{bat}$	Interfacing inductor of battery based VSC

$L_{fgsc}$	Interfacing inductor of GSC
$L_{fvsc}$	Interfacing inductor of PV-VSC
$L_m$	Mutual inductance of DFIG
$L_s$	Stator inductance of DFIG
$M$	Measuring point
$M_{ga}$	Filtering gain of the controller
$m_k$	Modulation index
$M_p$	Maximum peak overshoot
$n_{plpv}$	Number of parallel PV array
$n_{spv}$	Number of series PV array
$P_{bat}$	Battery power
$p_L$	Load power
$P_m$	Mechanical power
$P_{mppv}$	Maximum PV power
$P_{pv}$	PV power
$P_t$	DFIG power
$r$	Turbine blade radius
$R_l$	Resistance of sensor
$R_f$	Resistance of the ripple filter
$R_m$	Measuring resistance
$t_d$	Delay time
$TF_{DGI}$	Transfer function
$t_m$	DC voltage recover time
$T_m$	Mechanical torque
$t_r$	Rise time
$T_s$	Sample time
$u_{sabc}$	Unit templates of PCC/CCP voltages
$v_{a1}, v_{b1}, v_{c1}$	Reference PCC voltages
$V_{ADCm}$	Maximum ADC input voltage
$V_{bat}$	Battery voltage
$V_{batrf}$	Reference battery voltage
$v_{ccp}$	Standalone grid voltage
$v_{ccpa}, v_{ccpb}, v_{ccpc}$	Sensed local grid voltages
$V_{ccpd}, V_{ccpq}$	$DQ$ reference voltages
$V_D, V_Q$	$D$ -axis and $Q$ -axis voltages of FOC based RSC control
$V_{dc}$	DC-link voltage
$V_{dc1}$	DC-bus voltage across PV-VSC
$V_{dc2}$	Actual DC-bus voltage of GSC
$V_{dcerr}$	Error between reference and actual DC-link voltages
$V_{dcerr}$	DC-link error voltage (GSC)
$V_{DCREF}$	Reference DC link voltage
$V_{drt}$	Internal signal of $d$ -axis rotor voltage
$V_{drt}$ and $V_{qrt}$	Voltage references for RSC
$V_{gdpvf}$	PCC/CCP voltage magnitude
$v_{gfa}, v_{gfb}, v_{gfc}$	Reference PCC/CCP voltages
$V_{IGBT}$	IGBT voltage
$V_{mppv}$	Maximum MPPT voltage
$V_{oc}$	Open circuit voltage of single solar cell
$V_{odc}$	Output of the DC-DC converter voltage

$V_{offset}$	Offset voltage
$V_{out}$	Output voltage
$V_{pcca}, V_{pccb}, V_{pccc}$	Three phase PCC voltages
$V_{pccd}, V_{pccq}$	$D$ -axis and $q$ -axis PCC voltage
$V_{ph}$	Phase voltage
$V_{pv}$	PV voltage
$V_{qrt}$	Internal signal of $q$ -axis rotor voltage
$v_{raf}, v_{rbf}, v_{ref}$	Three phase reference voltage of FOC based RSC control
$V_{ref2}$	Reference DC-bus voltage of GSC
$v_s$	Stator voltage
$v_{sa}, v_{sb}, v_{sc}$	Three phase stator voltages
$V_{sen}$	Voltage to be sensed
$V_{sensor}$	Sensor voltage
$V_{st}$	Stator terminal voltage
$V_w$	Wind speed
$\beta$	Pitch angle
$\delta$	Adaptive feed forward term
$\Delta I_{mppv}$	Allowable current ripple
$\Delta V_{mppv}$	Voltage ripple
$\zeta_f$	Feedback term
$\theta_e, \theta_m$ and $\theta_r$	Electrical, mechanical and rotor angles
$\theta_{gf}$	Reference of grid forming converter angle
$\theta_{grid}$	Local grid angle
$\theta_{pcc}$ and $\theta_{ccp}$	PCC/CCP angle
$\theta_s$	Stator angle
$\theta_{slip}$	Slip angle of the DFIG
$\lambda$	Tip-to-speed ratio
$\rho$	Air density
$\omega_c$	Cut-off frequency
$\omega_m$	Actual rotor speed
$\omega_{mref}$	Reference rotor speed
$\omega_n$	Line frequency
$\omega_r$	Angular rotor speed
$\phi_s$	Sine angle difference [ $\sin(\theta_{pcc}-\theta_s)$ ]